

Theoretical Studies of Diffusion Mechanisms in Photon-Conducting Ceramic Materials

Neil J. Henson and Antonio Redondo

Global climate change is one of the primary environmental concerns of the twenty-first century, because the majority of the world's energy supply comes from fossil fuels, carbon dioxide emissions are believed to be a significant contributor. The carbon dioxide concentration has increased from its pre-industrial level of 280ppm to the current level of 365ppm with an annual growth of 1.7ppm.¹ Since any transition to alternative fuel sources is unlikely to occur in the near future, the only way reduce emissions significantly is to capture the carbon dioxide emissions and store them securely. This process is known as carbon sequestration.

A group of researchers at LANL is focusing on a couple of methods to perform sequestration efficiently. One approach involves the use of separation membrane technology to remove hydrogen from a mixed carbon dioxide/hydrogen exhaust gas stream such as that found in steam reforming of natural gas. Our experimental team has been able to synthesise ceramic membranes which have high hydrogen permeabilities at elevated temperatures. We are performing calculations on these materials in order to optimise their structure. The membranes are based on strontium zirconate (SrZrO_3) and strontium or barium cerate materials (Sr/BaCeO_3).

The crystal structure of SrZrO_3 is based on the perovskite structural group of materials. The idealised ABO_3 perovskite structure consists of corner-sharing BO_6 octahedra with A cations in the interstices in a cubic cell. In most perovskites, however, the octahedra rotate to better accommodate the size of the cations of type A. For example, in the SrZrO_3 structures, the polyhedra are tilted and the cell distorts to show orthorhombic symmetry (Figure 1).

In order to produce proton conductivity in this material, the zirconate is synthesized with a small amount of a trivalent cation dopant, M^{3+} , such as a lanthanide element or yttrium.

The cation substitutes onto the B cation site giving a charge imbalance that can be corrected by the formation of oxygen site vacancies ($\text{V}_\text{O}^{\cdot\cdot}$):

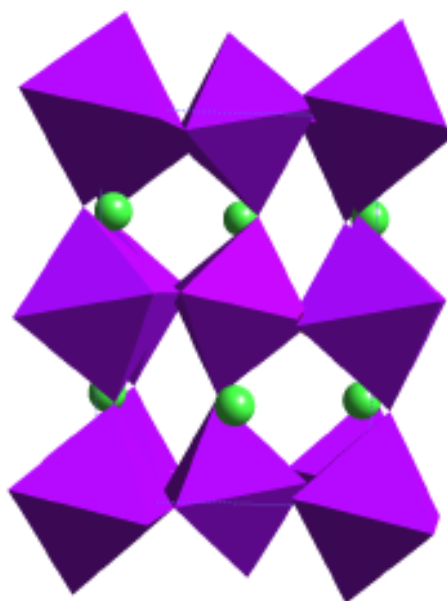
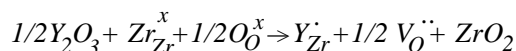
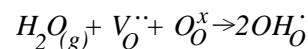


Figure 1: The structure of SrZrO_3 showing corner-sharing ZrO_6 octahedra (purple) and Sr^{2+} cations (green).

where A_A denotes the species A on site A, and \cdot represents a positive charge, \cdot represents a negative charge, and x represents no net charge. When the doped zirconate is exposed to water vapor, protons are incorporated into the structure via the formation of hydroxyl groups:



The primary conduction mechanism is thought to involve the hopping of protons between adjacent oxygen ions. In order to investigate this mechanism at the atomistic level, we have performed calculations on a number of different zirconate models.

A recent atomistic study on a similar system using shell model empirical potentials has been performed by Davies and co-workers². In this present study, we have employed quantum mechanical methods in periodic density functional theory using the total energy and molecular dynamics program, VASP.³

Initially a calculation was performed on the undoped SrZrO_3 structure to assess whether the techniques used are appropriate for this system. The electron-ion interaction is represented by ultrasoft pseudopotentials. The first calculation performed was carried out using only Bloch functions at the Γ -point corresponding to an electronic wavevector of $k = 0$. A full geometry optimisation was carried out at constant pressure on a single unit cell of the structure ($\text{Sr}_4\text{Zr}_4\text{O}_{12}$) and the results of the minimisation compared to experiment. Although it was found that a reasonable comparison with the experimental crystal structure was obtained from this calculation, convergence of the total energy with respect to the Brillouin

zone sampling was obtained by choosing the alternative wavevector $k = (1/4, 1/4, 1/4)$. This also improved the agreement with experiment. The comparison is shown in Table 1.

	a (Å)	b (Å)	c (Å)	v (Å ³)
experiment	5.796	5.817	8.205	270.3
theory	5.791	5.829	8.196	276.6

Table 1 : Comparison of experimental and calculated cell parameters(a, b, and c) and the cell volume (V).

The computed band gap of 3.9eV is considerably smaller than the experimental value of 5.4eV. However this is consistent with other calculations based on density functional theory.

Calculations were then performed on defect models of SrZrO_3 . To construct a defect model, a single Zr^{4+} ion was replaced by yttrium (Y^{3+}) and a proton was added. Since there are twelve oxygen atoms in the unit cell, there are a large number of possible binding sites and orientations for the hydroxyl group. To probe some of these possibilities, oxygen ions were selected at random and hydrogen atoms created at random orientations; each one of these generated configurations was minimised. The two most stable hydroxyl group positions are illustrated in Figure 2.

Comparing the energies of the two sites, it is found that the site bridging zirconium and yttrium octahedra (site 2) is more stable by about 14 kJmol^{-1} . Previous theoretical studies in similar perovskite structures have approached the problem of calculating the hopping behaviour of protons by performing molecular dynamics simulations. However, it has been found that the hopping process is sufficiently slow that it is difficult to capture the hopping event given the limited time of the simulation. In this study we employ the nudged elastic band method which is a method based on constrained energy minimisation to calculate hopping barriers. In this approach, a constrained trajectory is defined as lying between the two end-point minima by defining an arbitrary series of mid-point configurations using interpolation. The computed pathway is shown in Figure 3.

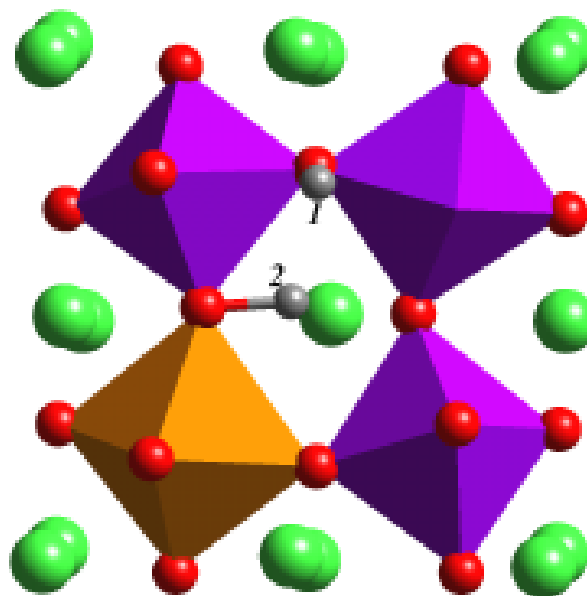


Figure 2: The most stable calculated -OH sites in an yttrium-doped SrZrO_3 model (labelled 1 and 2, yttrium in orange, hydrogen in gray).

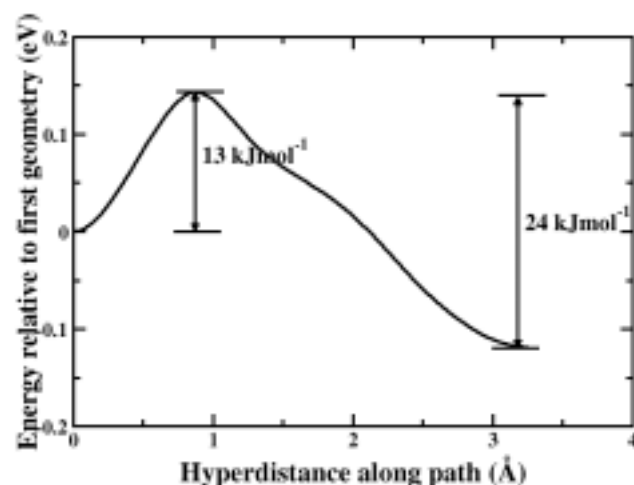


Figure 3: Energy profile of hopping pathway.

[1] C. D. Keeling, T. P. Whorf, M. Wahlen and J. van der Plicht, *Nature* **375**, 666-670 (1995).

[2] R. A. Davies, M. S. Islam and J. D. Gale, *Solid State Ionics* **126**, 323-335 (1999).

[3] G. Kresse and J. Hafner, *Phys. Rev. B* **47**, 558-561 (1993).

A U. S. Department of Energy Laboratory
This paper is a portion of LA-UR-00-1.

neil.henson@lanl.gov
redondo@lanl.gov

Los Alamos